Electronic Supplementary Material (ESI) for New Journal of Chemistry.

Supporting information

Preferred zinc modified melamine phytate for the flame retardant polylactide with limited smoke release

*Dong Wang, Yang Wang, Xuhui Zhang, Ting Li, Mingliang Du, Mingqing Chen and Weifu Dong**

* Corresponding author. E-mail: wfdong@jiangnan.edu.cn.

Key Laboratory of Synthetic and Biological Colloids, Ministry of Education, School of Chemical and Material Engineering, Jiangnan University, 1800 Lihu Road, Wuxi 214122, China

Figure S1. The solubility of divalent metal ion phytate in aqueous solution (0.1 g/mL) in different proportions.

Table S1. Formulations of PLA and PLA composites by mass fraction

Samples	PLA (wt%)	MPA (wt%)	MPACu (wt%)	MPAZn (wt%)	MPAMg (wt%)
Neat PLA	100	0	0	0	0
PLA/MPA_{20}	100	20	0	0	0
PLA/$MPACu_{20}$	100	0	20	0	0
PLA/$MPAZn_{20}$	100	0	0	20	0
PLA/$MPAMg_{20}$	100	0	0	0	20

Table S2. The Semi-quantitative Elemental Proportion of MPA and MPAR Measured by XPS

Samples	N: P: R^{2+} (At.%)
MPA	25.6: 6: 0
MPACu	19.8: 6: 0.75
MPAZn	23.3: 6: 0.92
MPAMg	26.3: 6: 0.3

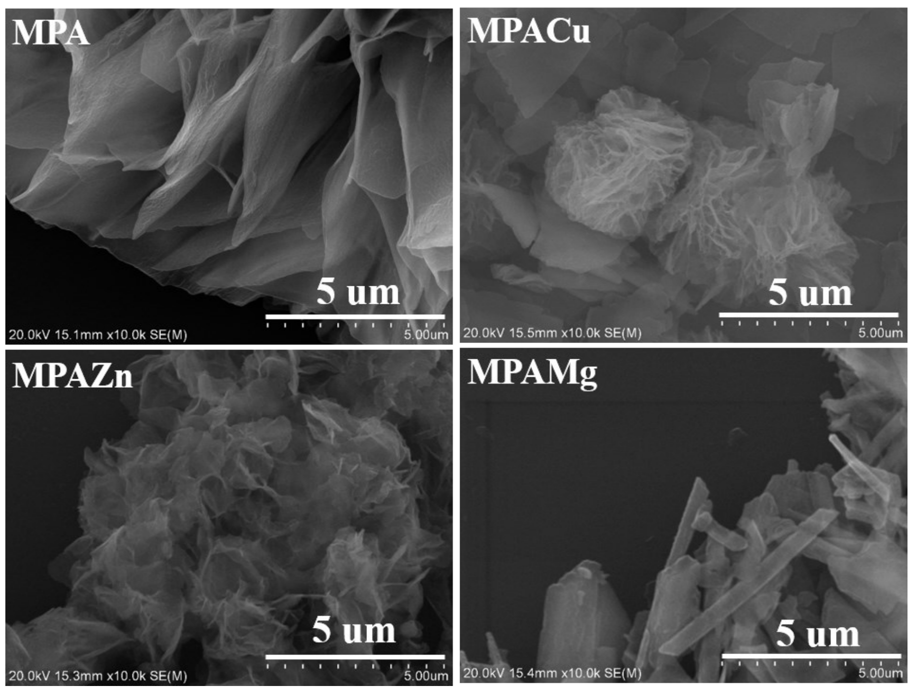

Figure S2. The representative SEM images of MPA and MPAR nanosheets before ball-milling.

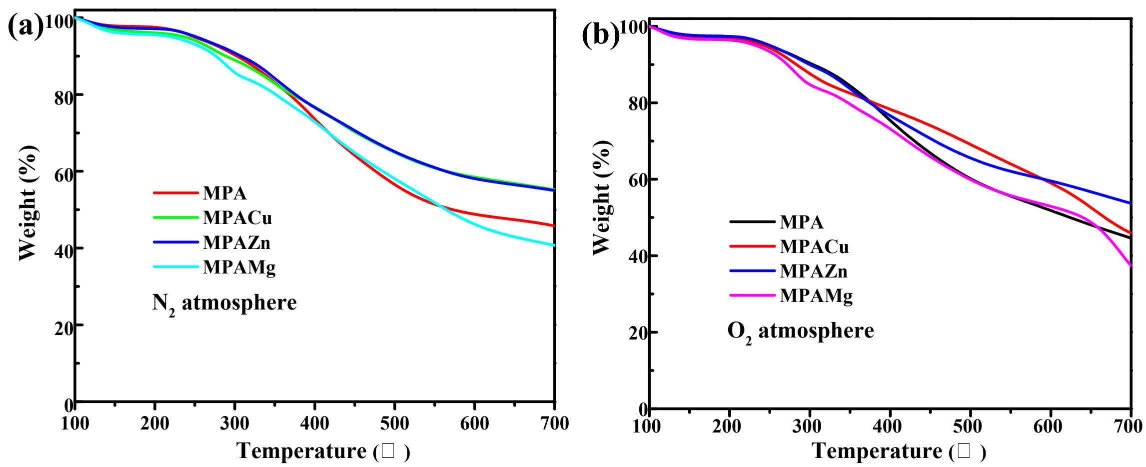

Figure S3. The TGA curves of MPA and MPARs under N_2 (a) or O_2 (b) atmosphere.

Table S3. Data of TGA for MPA, MPARs, PLA and PLA Composites under N_2 and O_2 Atmosphere

Samples	N_2 atmosphere			O_2 atmosphere		
	T_{onset} (°C)	Residual weight at 700 °C (wt%)		T_{onset} (°C)	Residual weight at 700 °C (wt%)	
		Experimental	Theoretical		Experimental	Theoretical
MPA	248.7	38.5	/	247.3	44.6	/
MPACu	236.7	55.2	/	241.7	45.9	/
MPAZn	251.7	55.0	/	250.3	53.7	/
MPAMg	220.7	40.7	/	232.3	37.4	/
Neat PLA	343.5	1.0	/	324.5	0.5	/
PLA/MPA_{20}	318.7	11.0	7.3	319.2	2.1	7.9
PLA/$MPACu_{20}$	326.4	10.3	10.0	325.2	6.5	8.1
PLA/$MPAZn_{20}$	312.9	9.7	10.0	312.3	6.3	9.4
PLA/$MPAMg_{20}$	301.8	10.0	7.6	297.8	4.4	6.6

S4

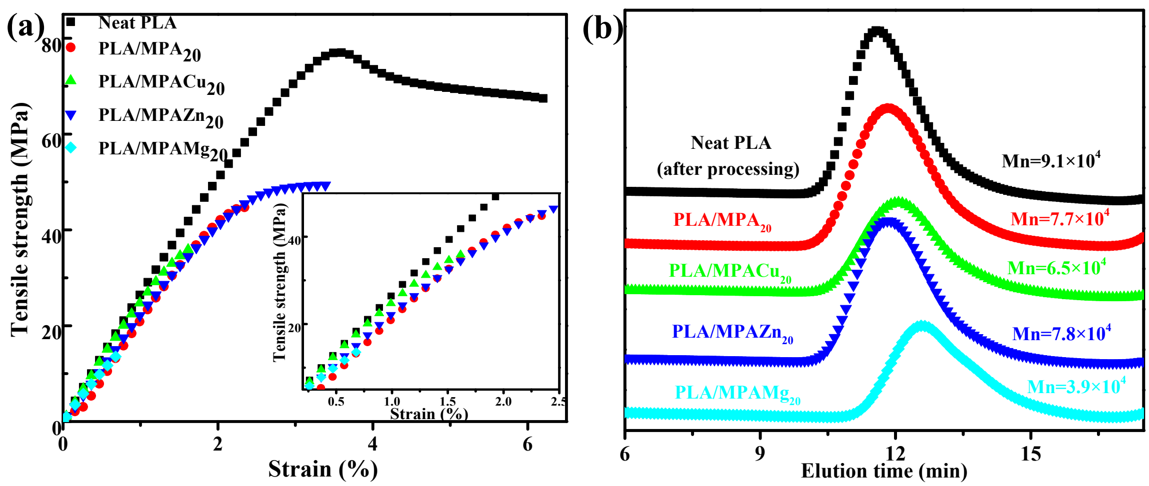

Figure S4. The typical stress-strain curves (a) and detected GPC traces (b) of PLA and PLA composites.

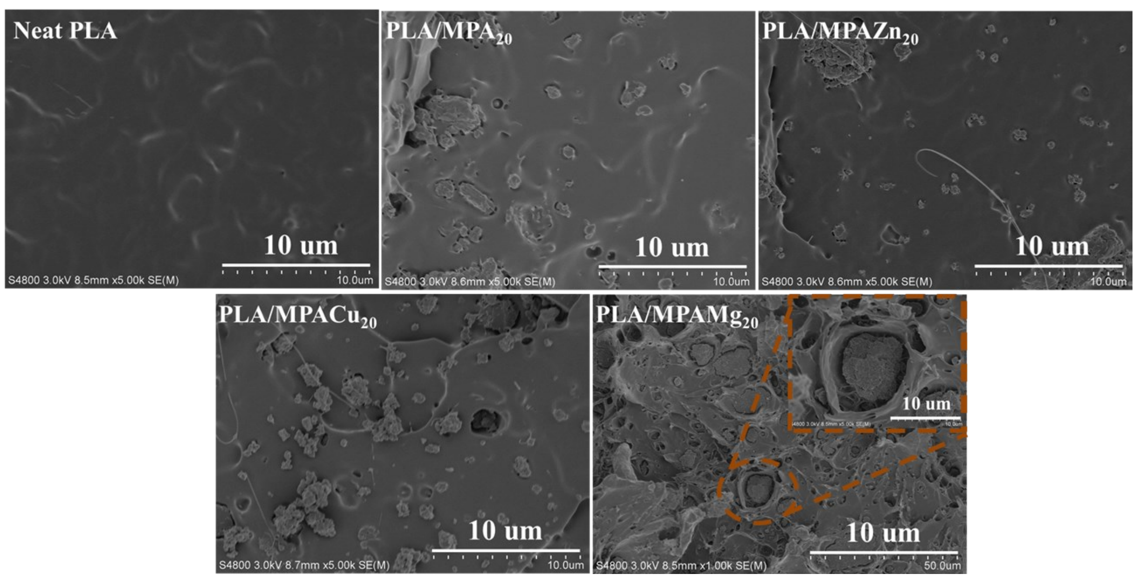

Figure S5. Representative SEM images of tensile fractured surfaces after tensile failure of neat PLA, PLA/MPA_{20}, PLA/$MPAZn_{20}$, PLA/$MPACu_{20}$, and PLA/$MPAMg_{20}$ films.

S5

Table S4. Mechanical Properties and Number-average Molecule Weights (*M*n) of Neat PLA and PLA Composites

Samples	Initial Young's modulus (MPa)	Tensile strength (MPa)	Elongation at break (%)	Number-average Molecule Weight (Daltons)
Neat PLA	2617.5±105.4	73.5±4.9	6.5±0.2	9.1×10^4
PLA/MPA_{20}	2513.4±168.4	45.3±0.7	2.4±0.1	7.7×10^4
PLA/$MPACu_{20}$	2537.5±144.9	35.2±1.0	1.8±0.1	6.5×10^4
PLA/$MPAZn_{20}$	2514.6±191.3	46.8±4.1	2.3±0.2	7.8×10^4
PLA/$MPAMg_{20}$	2119.2±168.5	10.7±4.2	0.7±0.1	3.9×10^4

Table S5. Combustion Data of PLA and PLA Composites in Cone Calorimeter Test

Sample	PLA	PLA/MPA_{20}	PLA/$MPACu_{20}$	PLA/$MPAZn_{20}$	$PLAMPAMg_{20}$
TTI (s)	58 ± 2	38 ± 1	38 ± 1	41 ± 1	44 ± 2
PHRR (kW/m^2)	333.3 ± 9.5	241.6 ± 6.3	258.3 ± 5.9	183.1 ± 2.8	171.5 ± 1.6
THR (MJ/m^2)	42.8 ± 1.5	35.9 ± 1.2	36.7 ± 0.7	33.8 ± 0.8	31.9 ± 1.0
TSP (m^2)	1.2 ± 0.1	17.1 ± 1.8	8.8 ± 0.6	3.2 ± 0.3	5.2 ± 0.4

Table S6. The Semi-quantitative Elemental Proportion of Char Residues for PLA Composites Measured by XPS

Samples	C(At.%)	O(At.%)	N(At.%)	P(At.%)	R^{2+}(At.%)
PLA/MPA_{20}	66.9	25.1	2.0	6.1	0
PLA/$MPACu_{20}$	44.9	34.3	4.0	13.7	3.0
PLA/$MPAZn_{20}$	45.8	34.1	4.5	12.8	2.7
PLA/$MPAMg_{20}$	59.4	25.1	8.3	6.3	0.6